Origin of phase contrast: insight from susceptibility, R2* and element imaging by LA-ICP-MS

A-M. Oros-Peusquens[1], A. Matusch[2], J. Lindemeyer[3], S. J. Becker[4], and N. J. Shah[1]
[1]Institute of Neuroscience and Medicine (INM-4), Research Centre Juelich, Juelich, NA, Germany, [2]INM-2, Research Centre Juelich, Germany, [3]INM-4, Research Centre Juelich, Germany, [4]ZCH, Research Centre Juelich

Introduction: Recent progress in susceptibility reconstruction from single or multiple phase images [1,2,3] has led to a better characterisation of this novel contrast in the brain. A surprisingly large anisotropy of the reconstructed susceptibility of white matter has been observed and is being discussed [4,5,6]. However, neither the source of anisotropy nor that of susceptibility contrast are fully understood. Differences between distributions of capillaries, iron content, exchange with and content of macromolecules, and myelin content, have been proposed as contributors to the phase contrast between white and grey matter in the brain [7,8,9]. Further, susceptibility anisotropy of myelin has been suggested as the source of the anisotropic susceptibility of white matter. A picture slowly emerges in which iron appears to be the main source of susceptibility contrast in grey matter and myelin density in the white matter. In addition, exchange with bound protons contributes to diminishing the phase contrast in fixed tissue [10]. With the aim of contributing to the clarification of the origin of phase and susceptibility contrast, we have investigated a post mortem rat brain with high-resolution (60 µm isotropic) MRI. For the very first time, to our knowledge, the MR-based phase, susceptibility and R2* maps are compared to complete, spatially resolved element analysis using LA-ICP-MS [11]. The element analysis was performed on two slices from the brain scanned with MRI and with a resolution similar to that of MRI.

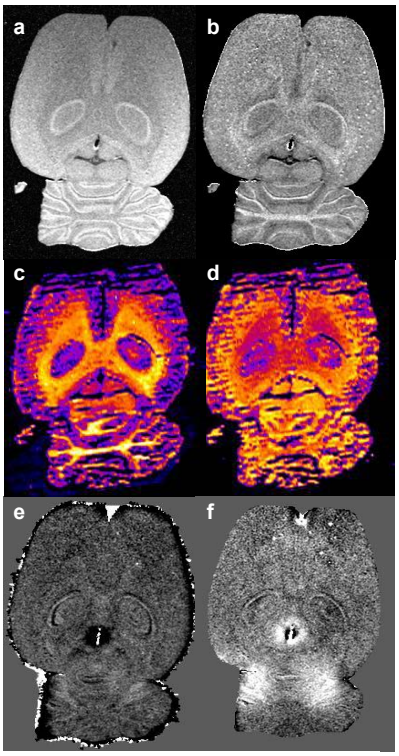

Fig. 1

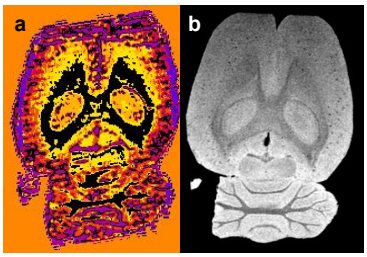

Fig. 2

Materials and methods: MRI was performed on a 7T Bruker/Siemens ClinScan animal scanner based on a 210 mm bore superconducting magnet (Magnex) equipped with a gradient coil with maximum gradient strength of 400 mT/m per axis and 170 µs rise time. RF excitation and reception was performed with a surface coil of 3 cm diameter. The brain of a male Wistar rat was investigated after storage in 6% formaldehyde solution for 14 months. For the MRI examination, the brain was placed in a plastic container of 2 cm diameter and 3 cm height filled with Fomblin® (perfluoro polyether, Solvay Solexis). The parameters of the dual-echo 3D gradient-echo sequence used for imaging included: TR=80 ms, TE=4.5ms and 14.5 ms, alpha=50 deg, 2 averages, FOV=31mm x 25mm, matrix=512x416, slice thickness 60 µm, 192 slices. Twenty separate scans were acquired over a period of 2 days and the complex data were averaged off-line using Matlab. After averaging, the phase images corresponding to each echo were unwrapped using PRELUDE (FSL) and the field map was calculated from a linear fit to the phase as a function of TE. The smooth contribution to the field variation was eliminated using a low-pass Gaussian filter with FWHM of 24x20 pixels. Susceptibility reconstruction was performed with an algorithm based on the method reported by de Rochefort et al. [2]. A single-exponential fit to the signal intensity delivered R2* and S0 (signal intensity at TE=0) maps. LA-ICP-MS measurements for two-dimensional (2D) imaging of biological tissues were performed by the line scanning ablation of thin cryocut tissue sections as described in [12]. The diameter of the focused laser beam during ablation was 100µum and the gap between lines 60µum. Quantification of analytical data was performed using matrix-matched home-made brain laboratory standards with known element concentration, measured together with the tissue samples under the same experimental conditions. Due to the multi-element capability of the novel LA-ICP-MS technique nearly all trace elements and minor elements were analyzed directly without any additional sample preparation in one measurement of the tissue section. We concentrate in the following on images of Fe and C, elements supposed to be markers of the leading contributions to phase and susceptibility contrast. The distribution of P instead of C as a marker of protein distribution has also been investigated and leads to very similar results.

Results and Discussion: Fig.1 shows a comparison of (semi)quantitative MR information (a,b,e,f: S0 [au], R2* [20-100] Hz, field map -2.8 to 3.4 Hz, susceptibility [au], respectively) with the distribution of carbon [counts/s] and iron [0 to 25ppm] (c,d) in a 40um thick slice. The closest matching slice from the MR data set was chosen by visual inspection, but accurate coregistration of the deformed slice with the 3D MR data set is difficult . Cluster analysis was performed using the distributions of 15 elements (among them Cu, Zn, Fe, Cr, Mn, C, P, Na, K, Pb) as independent components. The result of a k-means clustering analysis with 10 clusters is shown in Fig. 2a. TheMRI information which most closely displays the same structures is the mixed contrast image acquired at TE=14.5ms (Fig. 2b). Little resemblance is seen between the very flat susceptibility map and the richly featured distribution of elements. A quantitative analysis was performed using the intensity in small ROIs of the element distribution and trying to match them as closely as possible in the MR maps. From a ROI-based analysis with 6 ROIs placed in neighbouring homogeneous regions, good linear dependence of R2* on iron concentration was found, with a slope of 65 Hz/ppm. However, from visual inspection of Figs. 1 b and d, which differ in the distribution of contrast, either the dependence is not the same over the whole slice or other contributions to R2* are important. The correlation between R2* and concentration of C was poor. In the small number of homogeneous ROIs analysed, the dependence of the susceptibility on Fe and C concentrations was described reasonably well by a linear fit. The coefficients of the dependence incorporate the susceptibility of the compounds in which Fe and C are found in the tissue. The contributions were found to have the same sign (negative). However, a combination of the element distributions using the same coefficients as for the ROI-based fit would give rise to the susceptibility distribution more similar to that of C (Fig. 1c). The resemblance with either the reconstructed susceptibility map or the underlying field map is very limited. In conclusion, element analysis opens a unique path towards understanding the microscopic basis of susceptibility and phase contrast. A first attempt to interpret the susceptibility map as a linear superposition of Fe and C concentrations does not, however, seem realistic. Further elements and/or effects need to be included in the analysis, but this would ideally be performed on a voxel-by-voxel basis in coregistered data sets, such that a large number of data points from all regions is included. Work is in progress to obtain such 3D information and compare it with *in vivo* phase contrast. The final conclusion of our novel study is that, when a more complete picture is employed than the limited, ROI-based one, the field and susceptibility distributions does not closely match that of either Fe or C. A closer look at various aspects involved in this comparison is required – details of the susceptibility reconstruction on one hand, and significant influences from more elements and/or mechanisms on the other.

References: [1] Wharton et al., Neuroimage, 53(2):515-25 (2010); [2] de Rochefort et al., MRM, 63(1):194-206 (2010); [3] Shmueli et al., 62(6):1510-22 (2009); [4] Lee et al., PNAS, 107(11):5130-5 (2009); [5] Liu, MRM, 63(6):1471-7 (2010); [6] He et al., PNAS, 106(32):13558-63 (2009); [7] Duyn et al., PNAS, 104(28):11796-801 (2006); [8] Zhong et al., Neuroimage 40, 1561–1566., (2008); [9] Yao et al., Neuroimage, 44(4):1259-66 (2009); [10] Shmueli et al., MRM, 2010 Oct 6; [11] Becker, JS Inorganic Mass Spectrometry, Principles and Applications; Wiley, 2007. [12] Becker, JS et al. 2010, Mass Spectrom Rev 29,156.